Complexity Project
The Oslo Model

CID: 01874240

13th February 2023

Abstract: In this project non-equilibrium steady state is investigated through the Oslo model of a ricepile. The model is based on the one-dimensional Bak-Tang-Wiesenfeld (BTW) model, which describes the scale invariance of non-equilibrium systems by introducing the self-organised criticality [1]. The Oslo model of a ricepile is simulated in Python using Object-Oriented Programming (OOP). Multiple experiments are conducted on the simulation to investigate the behaviour of a ricepile and deduce the relationships between the size of the system, height of the system, cross-over time and avalanche sizes. The average height behaves linearly with the system size, but corrections to scaling are required for smaller systems. The cross-over time scales quadratically with the system size. The height probability distribution for different system sizes can be collapsed by assuming the Central Limit Theorem and using the measured standard deviation and mean of the total heights. The avalanche-size probability is log-binned and the distribution is collapsed using the avalanche-size exponents, τ_s and D. These parameters are measured using two procedures: avalanche-size probability and k'th moment analyses. The avalanche-size probability analysis gives $\tau_s = 1.546 \pm 0.019$ and $D = 2.175 \pm 0.082$. The k'th moment analysis returns $\tau_s = 1.542 \pm 0.050$ and $D = 2.134 \pm 0.013$. Both methods result in consistent values within the error range.

Word count: 2487 words in report.

1 Introduction

Most fields of physics describe the governing laws of isolated systems. These systems can be recreated under laboratory conditions, but most systems in Nature are not isolated. These systems have a flux of energy or mass, which indicates that they are not in equilibrium. However, these systems can still be described by laws of physics if they are in a steady state, i.e. if the net flux or another quantity is constant.

The field of Complexity aims to describe these non-equilibrium steady state systems by analysing mechanisms which generate scale-free behaviours. One of the mechanisms is self-organised criticality (SOC), which was proposed by Bak, Per and Tang, Chao and Wiesenfeld, Kurt in 1987 [1]. They argued that minimally stable systems react to small perturbations by self-organising and reaching a critical point - recurrent configurations, which behave like attractors of the system. At a critical point, observable quantities can be described by scale-free power-law functions.

1.1 The Boundary-Driven One-Dimensional Oslo Model

Consider a one-dimensional lattice of size L. This lattice represents a ricepile with L sites, $i = 1, 2, ..., L$. The lattice has a boundary on the left, but no boundary on the right, meaning that the grains of rice can only leave the system at site $i = L$. The system is driven by adding a grain of sand to the left-most site ($i = 1$). It topples to the neighboring site if the the threshold slope is exceeded. The site's slope, z_i, is defined as the difference between two neighboring sites, $h_i - h_{i+1}$. In this model, the threshold slope of site i, z_i^{th}, can have two values: 1 or 2. Initially, the threshold slope of each site is chosen randomly between the two values with equal probability. This means that if the height of site i, h_i, is larger than the nearest site's height, h_{i+1} by more than 1 or 2, the site i must 'relax' and the added grain topples to site $i + 1$. The first toppling can cause another site to relax, hence the avalanche propagates until all sites have a slope $z_i < z_i^{th}$. If site $i = L$ has to topple, the grain leaves the system. After each relaxation, site i has a new threshold slope value, which is chosen randomly between 1 or 2. The algorithm of the Oslo model is described in *Complexity and Criticality* by K. Christensen and Nicholas R. Moloney.

There is a finite number of stable configurations, $\mathcal{S}$. These can be divided into two types: transient, $\mathcal{T}$, and recurrent, $\mathcal{R}$. The system's initial stable configurations are transient. Once a sufficient number of grains are in the system, the added grain will topple down until it leaves the system. This means that the net flux of grains becomes zero and the site configuration is called the recurrent configuration. Due to the threshold values changing between two values, there are several recurrent configurations.

This model can be used to describe natural granular systems which are governed by friction. The added grain creates an inward flux of potential energy. The threshold slope is the threshold friction between grains. By exceeding the threshold friction, the relaxations begin and the added potential energy is converted to kinetic energy which then dissipates.

2 Implementation of the Oslo Model

The Oslo model was simulated in Python using Object-Oriented Programming (OOP). It contains one class called `Oslo` and takes three variables: the system size L, a list of the threshold slopes z^{th}, and a list of probabilities of these threshold slopes p. For convenience, $z^{th} = [1, 2]$ and $p = [0.5, 0.5]$ by default. The class contains several functions: following the Oslo algorithm, forcing the system to reach its first recurrent configuration, measuring the height of the system,

measuring the threshold slopes of each site, measuring the avalanche sizes, and animating the simulation for visualisation.

For the investigation purposes, the experimental data is analysed by finding its fit function. The fit functions are found by using `numpy.polyfit` or `scipy.optimize.curve_fit` and the errors of the fitting parameters are estimated by finding the square root of the covariance matrix diagonal elements.

2.1 Testing the Simulation

The simulation was examined via several tests, including measuring the pile height and comparing them with the given values. For system sizes $L = 16$ and $L = 32$, the average height is 26.5 and 53.9, respectively. These values match the values given in *Complexity Project Notes*, meaning the simulation works as expected.

The simulation can also be used to compare the BTW and the Oslo model by measuring the system's height over time (time is measured in number of grains added), shown in Figure 1A. As expected, the BTW reaches its only recurrent configuration while the Oslo model has several.

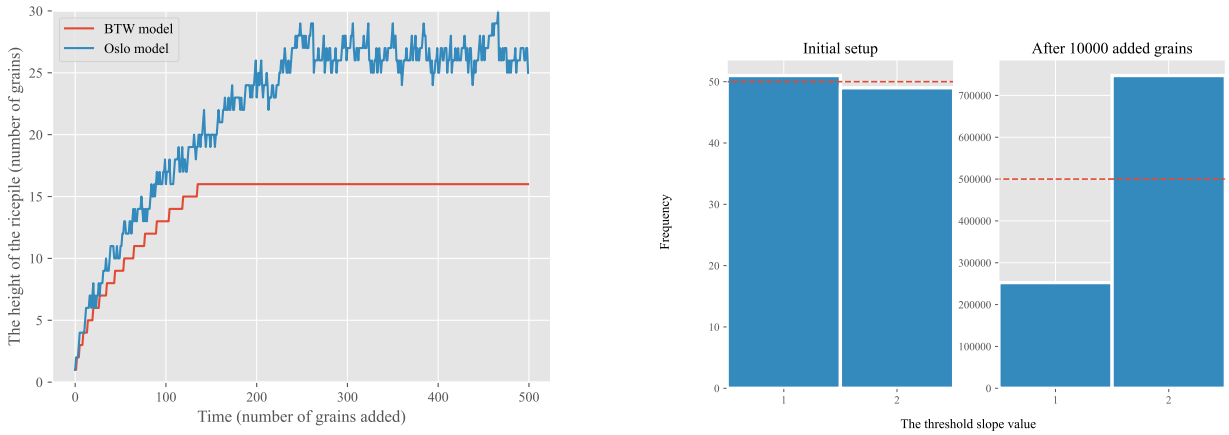

(A) (B)

Figure 1: Testing the Oslo model simulation. Fig. 1A: The comparison between the BTW and the Oslo models with $L = 16$. The BTW model reaches its only recurrent configuration, where each site's slope is 1. The Oslo model has many recurrent configurations due to the changing threshold slope for each site. Fig. 1B: A histogram of threshold slopes of each site for the $L = 100$ Oslo model. The red dotted line represents the expected frequency. The initial setup shows that the z_i^{th} is chosen between two values with almost equal frequency. After driving the model 10,000 times, the $z_i^{th} = 2$ appears more often.

Moreover, the frequency of the threshold slope values of each site was investigated. The histogram is shown in Figure 1B. As demonstrated, the frequency of the threshold values upon initialisation is approximately equal between the two values. However, after running the Oslo algorithm, the threshold value $z_i^{th} = 2$ is more frequent. This is expected as sites with $z_i^{th} = 2$ are less likely to be relaxed, hence their threshold value updates less frequently.

3 The Height of the Pile

The height of the pile, $h(t; L)$, is defined as the height of site $i = 1$. Before completing tasks specified in *Complexity Project Notes*, systems of sizes $L = 4, 8, 16, 32, 64, 128, 256$ were driven 600,000 times. For each system size the following quantities were saved in a separate file: the total height, avalanche sizes and the 'criticality condition'. The 'criticality condition' is a variable which begins as False and becomes True when the first grain leaves the system. This variable is needed for the investigation of the cross-over time.

3.1 Total Height of the Pile vs. Time

The measured total height as a function of time, t, is shown in Figure 2A. The same data can be smoothed by the Savitzky–Golay filter [3] and plotted on a logarithmic scale as shown in Figure 2B. The system sizes $L \gg 1$ have the same progression with time until a recurrent configuration is reached. The bigger the system size, the more time is required to reach a steady state.

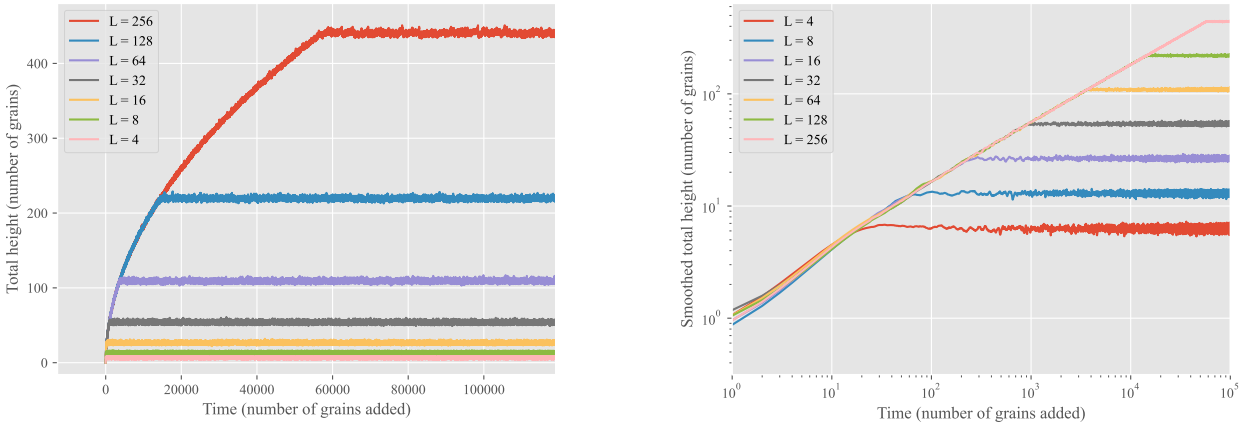

(A) (B)

Figure 2: The total height of the pile against time measured in number of added grains. Fig. 2A: Total height of piles with $L = 4, 8, 16, 32, 64, 128, 256$. The systems' heights exponentially increase until they reach the recurrent configurations. The maximum total height is dependent on the system size. Fig. 2B: The same data represented on a log scale after applying the Savitzky–Golay filter [3] for smoothing the data.

To further investigate transient and recurrent configurations (specifically for system sizes $L = 4, 8$), the time at which the first grain leaves the system is measured. The result is shown in Figure 3, where the dotted line represents the transient, and the solid line represents the recurrent configurations.

3.2 Cross-Over Time

The cross-over time, $t_c(L)$ is defined as the number of grains added to the system before a grain leaves the system for the first time. $\langle t_c(L) \rangle$ is the cross-over time averaged over the system size L. For the purposes of this experiment, 10 Oslo models were created of each system size. The numerical measurements of $\langle t_c(L) \rangle$ are shown in Figure 4. The uncertainty of the data-points are found by calculating the standard deviation of all recorded cross-over times for each size. It

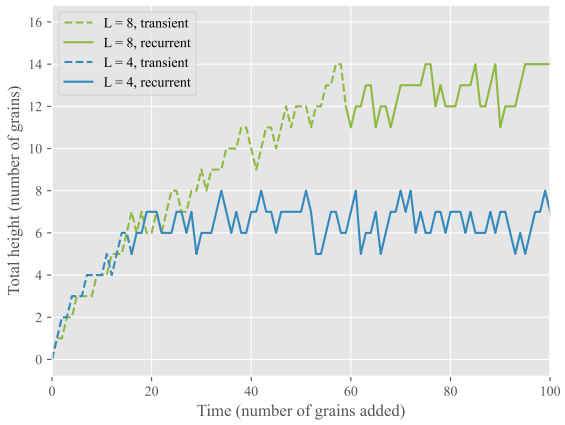

Figure 3: Total height of the pile against time for $L = 4, 8$ ricepiles. The dashed lines represent the systems being in transient configurations. The solid lines represent the systems being in recurrent configurations.

is evident that the relationship between $\langle t_c(L) \rangle$ and L can be described by a quadratic function $(ax^2 + bx + c)$, and the following parameters were measured by `numpy.polyfit`:

$$\begin{aligned} a = &\quad 0.869 \pm 0.003 \\ b = &\quad -3.064 \pm 0.685 \\ c = &\quad 34.742 \pm 7.286 \end{aligned}$$

The quadratic function fits the data well given that the uncertainties of the parameters are significant.

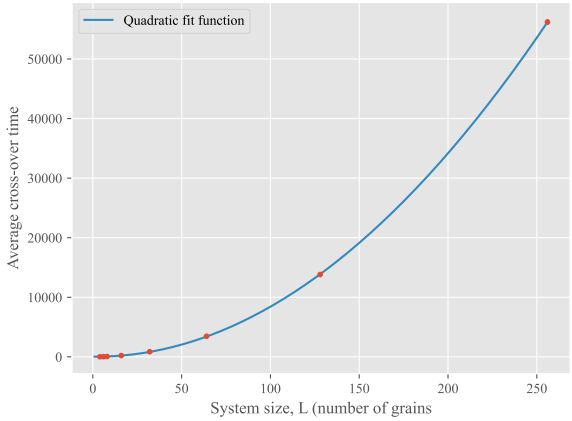

Figure 4: Numerically measured average cross-over time, $\langle t_c(L) \rangle$, vs. size of the system , L. The $\langle t_c(L) \rangle$ is estimated by creating 10 Oslo models of each size $(L = L = 4, 8, 16, 32, 64, 128, 256)$, measuring t_c and averaging it over system size. The error bars of data points are insignificant. The average cross-over time behaves as $\langle t_c(L) \rangle \propto L^2$.

3.3 The Average Total Height and Cross-Over Time

For systems with $L \gg 1$ in a steady state, the pile can be approximated as a right triangle with a constant slope. The constant slope indicates that the average height scales as $\langle h(t; L) \rangle \propto L$.

The cross-over time can be estimated as the number of grains needed in the system for the right triangle to form, i.e. it is equivalent to the area of the triangle. This means that the average cross-over time scales as $\langle t_c(L) \rangle \propto L^2$. This relationship was proven in Section 3.2.

3.4 Data Collapse For Height

The processed height is measured by averaging the height over different realisations. In this project, 5 Oslo models of each size are used to process the data. The result on a logarithmic plot is shown in Figure 5A. As discussed in Section 3.3, the average height and the average cross-over time scale as $\langle h(t;L) \rangle \propto L$ and $\langle t_c(L) \rangle \propto L^2$. Therefore, by dividing the measured processed height by L and time, t, by L^2 the data can be collapsed. Mathematically, this can be expressed as:

$$\tilde{h}(t;L) = L\mathcal{F}(\frac{t}{L^2}), \tag{1}$$

where $\mathcal{F}$ is the scaling function.

The progression of transient into recurrent configurations is demonstrated in Figure 5B. It is much sharper for system sizes $L \gg 1$. According to the graph, in the thermodynamic limit the behaviour of $\mathcal{F}$ can be summarised as:

$$\mathcal{F} \propto \begin{cases} L^{0.506}, & \text{for } x < 1 \\ \text{constant}, & \text{for } x > 1 \end{cases}, \tag{2}$$

where the power parameter was estimated via `scipy.optimize.curve_fit`.

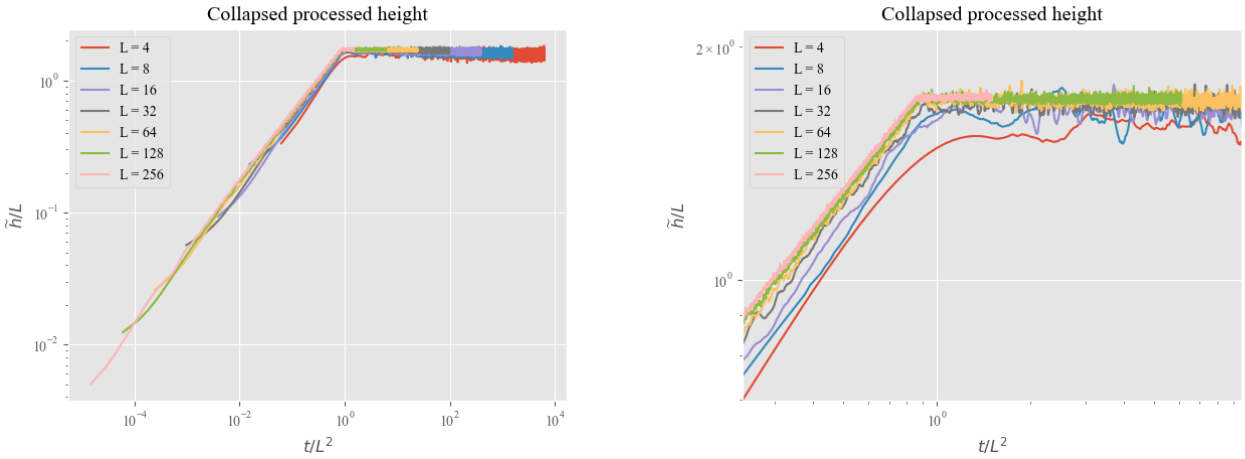

(A) (B)

Figure 5: The collapsed processed height of system sizes $L = 4, 8, 16, 32, 64, 128, 256$. The data was smoothed by using the Savitzky–Golay filter. Fig. 5A: The processed height, $\tilde{h}(t;L)$, divided by system size, L, plotted against t/L^2. The data collapses onto a single curve. Fig. 5B: The same graph zoomed in a region where the transient transform into the recurrent configurations. The $L = 256$ system has a sharp transition, therefore it was used to determine the behaviour of $\mathcal{F}$.

3.5 Signs of Corrections to Scaling

As mentioned in Section 3.3 the average height of the pile is proportional to the size of the system in a steady state ($t > t_c$). In order to evaluate this scaling behaviour, $\langle h(t;L) \rangle$ was

plotted. Figure 6A demonstrates that the relationship seems to be linear. However, if $\frac{\langle h(t;L)\rangle}{L}$ is plotted as shown in Figure 6B, the graph indicates that corrections to scaling for small L are required. Therefore, the average height can be expressed as:

$$\langle h(t;L)\rangle_t = a_0 L \left(1 - a_1 L^{-\omega_1} + a_2 L^{-\omega_2} + \ldots\right), \tag{3}$$

where a_i and ω_i are constants that need to be evaluated. For the purposes of this project, only the first order corrections were measured using `scipy.optimize.curve_fit`, giving the following results:

$$\begin{aligned} a_0 &= \quad 1.745 \pm 0.004 \\ a_1 &= \quad 0.187 \pm 0.004 \\ \omega_1 &= \quad 0.479 \pm 0.024 \end{aligned}$$

In the thermodynamic limit, as $L \to \infty$, the average slope $\frac{\langle h(t;L)\rangle_t}{L} \to a_0$, as expected.

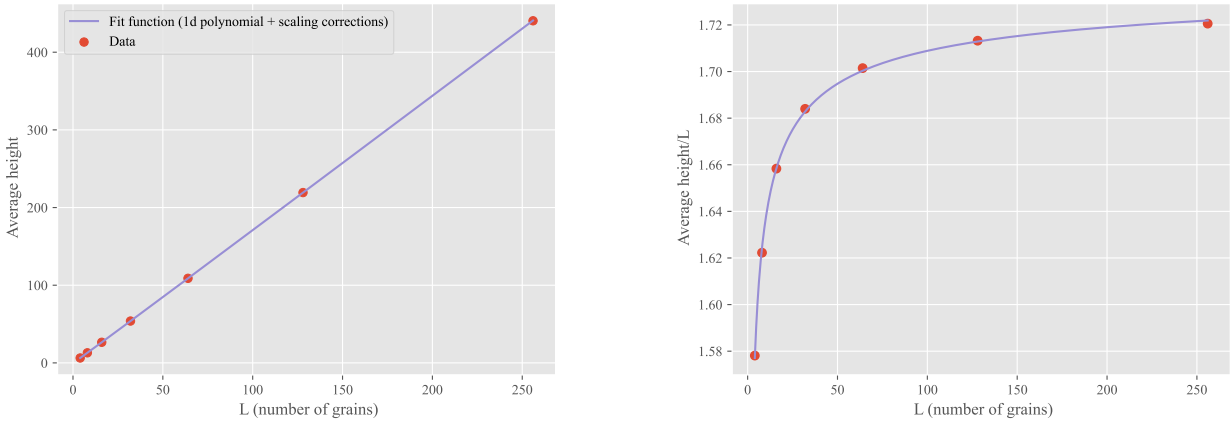

(A) (B)

Figure 6: The average height for system sizes $L = 4, 8, 16, 32, 64, 128, 256$ plotted against L. Fig. 6A: The relationship between $\langle h(t;L)\rangle$ appears to be linear. Fig. 6B: The $\langle h(t;L)\rangle/L$ plotted against L. The graph indicates that corrections to scaling are required for smaller systems.

3.6 Standard Deviation

The standard deviation of the average total height, σ_h, on a logarithmic scale is shown in Figure 7A, indicating that it follows a power function given as:

$$\sigma_h = \alpha L^{\beta}, \tag{4}$$

where α and β are constants to be determined. By using `scipy.optimize.curve_fit` these constants were found to be:

$$\begin{aligned} \alpha &= \quad 0.582 \pm 0.004 \\ \beta &= \quad 0.240 \pm 0.002 \end{aligned}$$

In the limit of $L \to \infty$, the standard deviation $\sigma_h \to \infty$ due to the power-law function. In order to check whether any corrections to scaling are needed, $\frac{\sigma_h}{\alpha L^{\beta}}$ was plotted in Figure 7B. All values are approximately equal to 1, which means that there are no corrections to scaling.

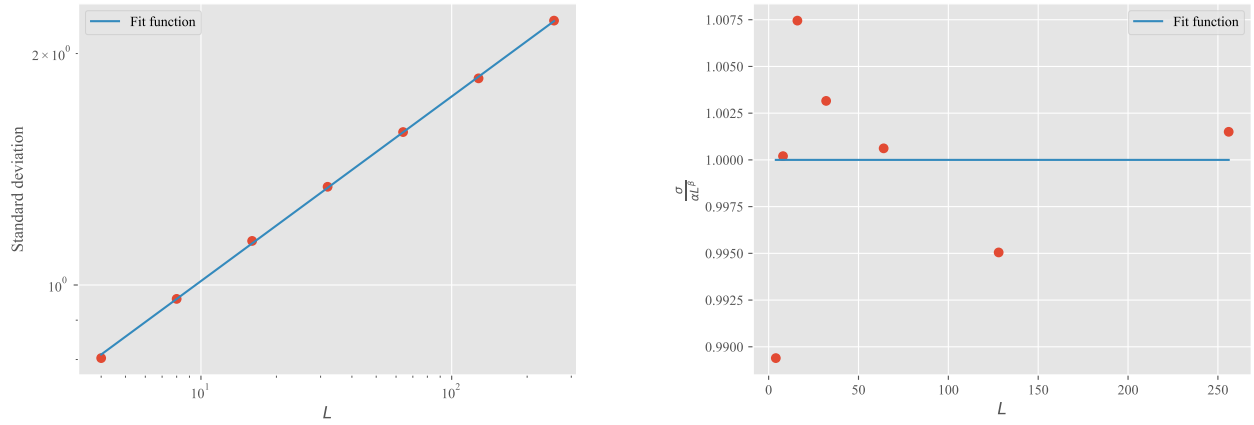

(A) (B)

Figure 7: Investigating the standard deviation of the total height, σ_h, of system sizes $L = 4, 8, 16, 32, 64, 128, 256$. Fig. 7A: The relationship between σ_h and L follows a power-law function as $\sigma_h = 0.582L^{0.240}$. Fig. 7B: $\sigma_h/(0.582L^{0.240})$ plotted against L. The graph demonstrates that no corrections to scaling are required as all values are ≈ 1.

3.7 Height Probability $P(h; L)$

The Central Limit Theorem (CLT) states that the distribution of a random variable approaches a normal distribution (or a Gaussian) as the sample size approaches infinity [4]. This statistical concept can be applied to the probability distribution of the total height, $P(h; L)$ as the slope of each site, z_i, is assumed to be a random variable with finite variance and the total height is $h = \sum_{i=1}^{L} z_i$. This assumption also leads to a scaling of the variance (σ_h^2) which follows the power-law function.

The measured height probability of steady-state systems is shown in Figure 8. The data points were fitted by a Gaussian distribution which is given by:

$$\mathcal{N}(x) = \frac{1}{\sqrt{2\pi\sigma^2}} \exp\left(-\frac{(x-\mu)^2}{2\sigma^2}\right), \tag{5}$$

where μ is the mean and σ is the standard deviation of the distribution. According to Equation 5, the height probability can be collapsed by multiplying $P(h; L)$ with σ_h and by shifting and re-scaling the heights as $\frac{h-\mu}{\sigma_h}$. Mathematically,

$$\sigma_h P = \mathcal{P}\left(-\frac{X}{2}\right) = \frac{1}{\sqrt{2\pi}} \exp\left(-\frac{X}{2}\right), \tag{6}$$

where $\mathcal{P}$ is the scaling function for $P(h; L)$ and

$$X = \frac{h-\mu}{\sigma_h} \tag{7}$$

This procedure was performed on the data and the result is shown in Figure 9. The collapse appears to be 'rough' because there are some deviations for each system size. This means that the validity of the assumption that z_i is a random variable should be questioned. z_i is highly dependent on the neighboring sites as a relaxation can cause z_i to change, therefore invalidating the Gaussian approximation.

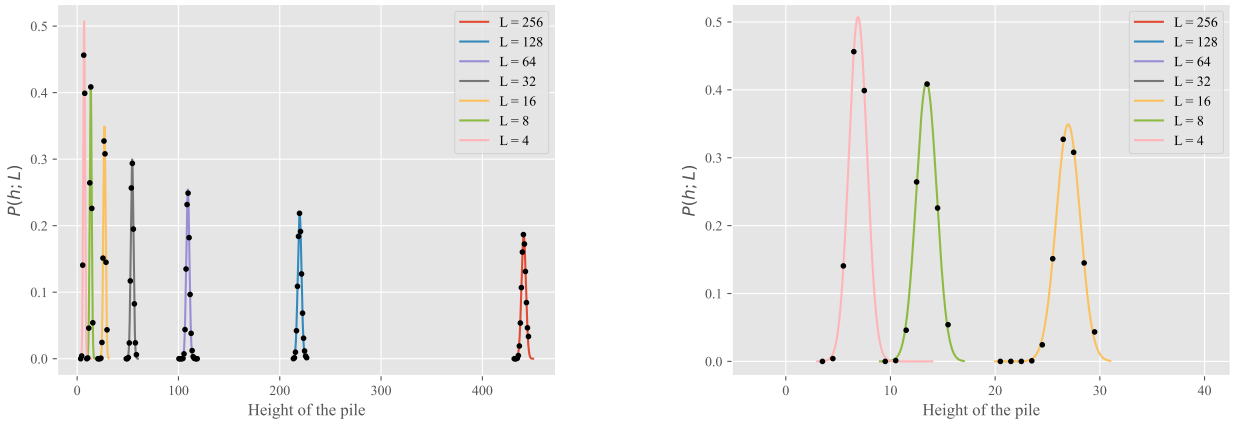

(A) (B)

Figure 8: The height probability, $P(h; L)$, plotted against total height, h. Fig. 8A: $P(h; L)$ for $L = 4, 8, 16, 32, 64, 128, 256$. The curves are assumed to be Gaussian. Fig. 8B: A zoomed in version of the same plot to illustrate the goodness of Gaussian fit. All data points lie on the fit function.

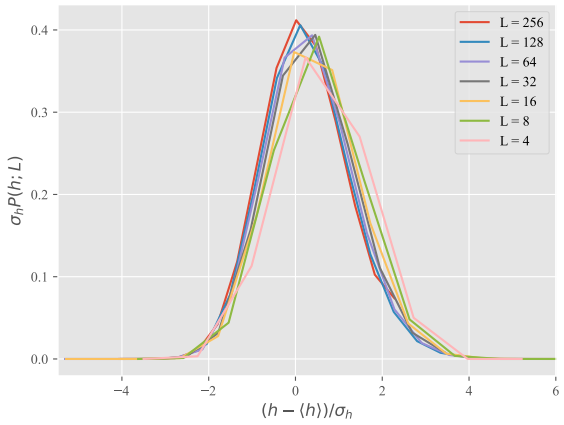

Figure 9: The collapsed height probability. The probabilities are multiplied with the standard deviation. The heights are shifted and scaled as $(h - \langle h \rangle)/\sigma_h$. The collapse seems to be invalid because of the small deviations for each system size.

The theoretical prediction can be tested via the Kolmogorov-Smirnov test. This test allows to perform a comparison between a Gaussian distribution and the experimental data [5]. The test returns a statistical variable which demonstrates the invalidity of the theoretical prediction, i.e. its value should be $< 1\%$ in order to statistically verify that the distribution is Gaussian.

4 The Avalanche-Size Probability $P(s; L)$

The avalanche size, s, is defined as the total number of toppled grains after a single grain is added. The avalanche sizes for system sizes $L = 4, 8, 16, 32, 64, 128, 256$ in a steady state were measured after adding 500,000 grains. The result for $L = 256$ is shown in Figure 10A, where a noisy tail can be observed, implying that the statistical analysis of this region is poor. The data binning algorithm can be used to reduce the noise.

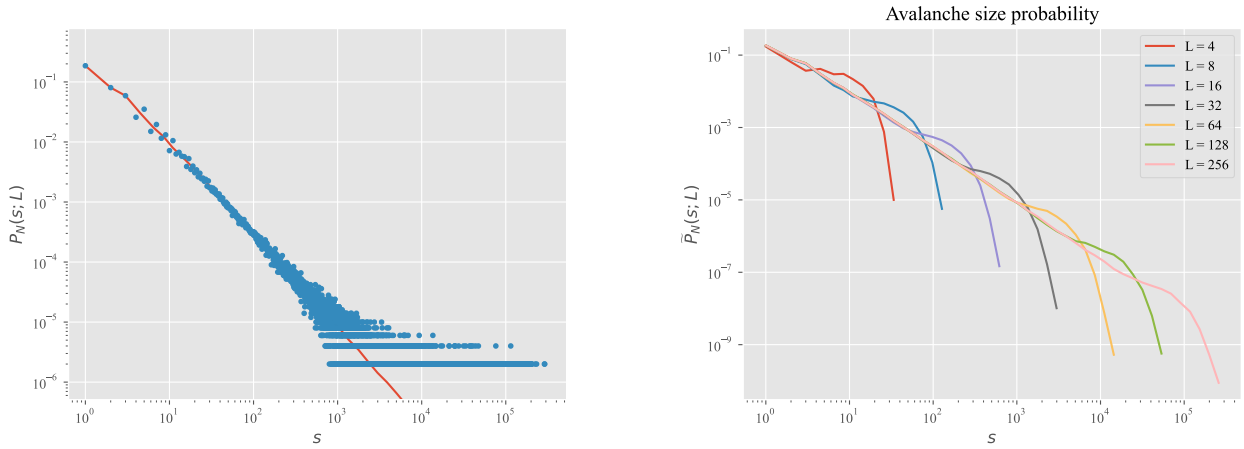

(A) (B)

Figure 10: Investigating the avalanche-size probability. Fig. 10A: The blue data points represent the probability of avalanche sizes for $L = 256$ plotted against the avalanche size. The noisy tail can be observed, hence log-binnnig procedure is performed. Fig. 10B: The log-binned avalanche-size probability for $L = 4, 8, 16, 32, 64, 128, 256$. The curves have a characteristic bump before decaying rapidly and reaching the cutoff avalanche size.

The data binning is performed by dividing the avalanche sizes into bins of exponentially increasing width. Consider dividing the avalanche sizes, s, into bins labelled $j = 1, 2, ...$ The width of each bin corresponds to the interval $[a^j, a^{j+1}]$, where $a > 1$. By defining the normalized avalanche size probability as:

$$P_N(s; L) = \frac{\text{No. of avalanches of size } s \text{ in a system of size } L}{\text{Total no. avalanches } N}, \tag{8}$$

the log-binned avalanche size probability is:

$$\tilde{P}_N\left(s^j\right) = \frac{\text{No. of avalanches in bin } j}{N \Delta s^j}, \tag{9}$$

where

$$\Delta s^j = s^j_{\min} - s^j_{\max} + 1, \tag{10}$$

and $s^j_{\min\,/\,\max}$ is the maximum/minimum avalanche size in bin j.

The log-binned probability is shown in Figure 10B with $a = 1.3$. The noise is reduced, however the information about the avalanche sizes is lost. The curves also display a characteristic bump before a rapid decay of the probability. The bump is related to grains leaving the system at site $i = L$.

4.1 Data Collapse for $P(s; L)$

The log-binned probability can be collapsed by using the finite-size scaling ansatz:

$$\tilde{P}_N \propto s^{-\tau_s} \mathcal{G}(s/s_c) \text{ for } L \gg 1, s \gg 1, \tag{11}$$

$$s_c(L) \propto L^D \text{ for } L \gg 1, \tag{12}$$

where $\mathcal{G}$ is the scaling function, τ_s is the avalanche-size exponent, D is the avalanche dimension, and s_c is the cutoff avalanche size.

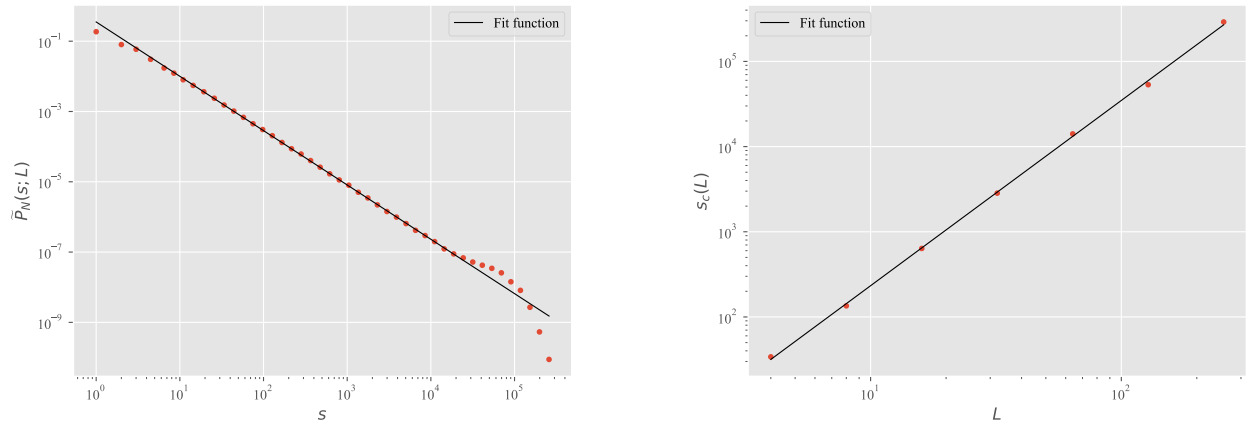

(A) (B)

Figure 11: Estimating the avalanche-size exponent, τ_s, and the avalanche dimension, D. Fig. 11A: The red datapoints represent the log-binned avalanche size probability for $L = 256$. The black line is the fit function performed on a region before the characteristic bump and its gradient is related to τ_s. Fig. 11B: The cutoff avalanche sizes plotted against system sizes. The black line is the fit function which gradient corresponds to D.

The validity of Equation 11 can be checked by collapsing the data. The characteristic bumps can be adjusted vertically and horizontally by multiplying the probability by s^{τ_s} and dividing the avalanche sizes by the cutoff avalanche size.

The avalanche-size exponent was approximated by analysing the probability in a region before the bump. The curve behaves as $\tilde{P}_N \propto s^{-\tau_s}$ and τ_s is its gradient on a log scale. `numpy.polyfit` works best for estimating the gradient. The plot of a fit function for $L = 256$ is shown in Figure 11A with $\tau_s = 1.546 \pm 0.019$.

The avalanche dimension was approximated by using the same procedure and using Equation 12. The biggest avalanche size, s_c, for each L against the system size L is shown in Figure 11B, where `numpy.polyfit` estimated the gradient to be $D = 2.175 \pm 0.082$.

Using the estimated parameters, the data collapse is performed and the resulting curve is shown in Figure 12B. The data collapses onto a single curve with good precision, thus justifying the ansatz given in Equation 11. However, the collapse is not perfect, as $P(s; L)$ for $L = 4$ deviates from the others by a small amount. This means that the slope of avalanche-size

probability is dependent on the system size and hence more analysis on the parameters is needed.

The scaling describes the behaviour of the avalanches. The avalanches are the system's response to an addition of a grain, i.e a response to an external perturbation. Furthermore, the D and τ_s exponents can be numerically calculated by executing the k'th moment analysis explained in Section 4.2.

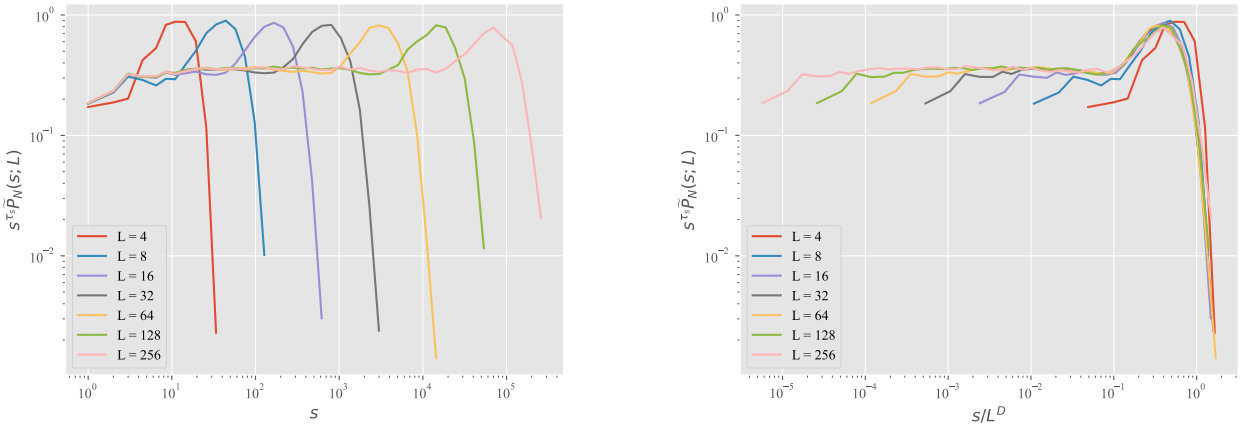

(A) (B)

Figure 12: A demonstration of the collapsing procedure for $\tilde{P}_N$. Fig. 12A: Aligning the characteristic bumps vertically by scaling the y-axis as $s^{\tau_s}\tilde{P}_N$. Fig. 12B: Aligning the characteristic bumps horizontally by scaling the x-axis as s/L^D. The data collapses onto a single curve.

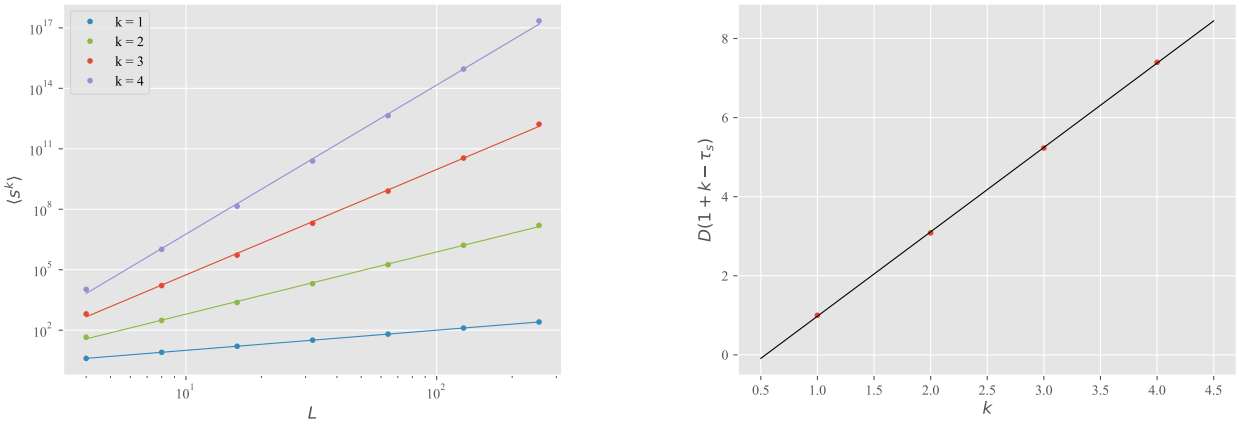

(A) (B)

Figure 13: Analysing the k'th moment. Fig. 13A: The average k'th moment for $k = 1, 2, 3, 4$ plotted against system size L. The curves follow the power-law functions and their gradients correspond to the avalanche-size exponents, τ_s and D. Fig. 13B: A plot of the curves' gradients vs. k. The slope corresponds to D and the k-axis intercept is related to τ_s.

4.2 k'th moment analysis

Define the average avalanche size $\langle s^1 \rangle$ as the first moment of $P(s; L)$. Then, the k'th moment, $\langle s^k \rangle$, is given by:

$$\langle s^k \rangle = \lim_{T \to \infty} \frac{1}{T} \sum_{t=t_0+1}^{t_0+T} s_t^k \propto L^{D(1+k-\tau_s)}, \tag{13}$$

where s_t is the avalanche size at time t and t_0 is time after the system reached recurrent configurations.

In this project, $k = 1, 2, 3, 4$ moments were numerically measured. These moments vs. system size L are shown in Figure 13A. The gradient of each curve on a log scale can be approximated with the use of `numpy.polyfit`. Equation 13 shows that the gradient corresponds to $D(1 + k - \tau_s)$. The estimated slopes were plotted against k and the result is shown in Figure 13B. The avalanche dimension was found by measuring the slope of this curve and `numpy.polyfit` returned $D = 2.134 \pm 0.013$. The avalanche-size exponent is the intercept with the k-axis +1, which was calculated to be $\tau_s = 1.542 \pm 0.050$. Both values are consistent with what was found in Section 4.1.

5 Conclusion

This project investigates the boundary-driven one-dimensional Oslo model. The model displays self-organised criticality after a system reaches a non-equilibrium steady state. In this state, the behaviour of the total pile height and the avalanches can be explained by scale-free power-law functions.

In particular, the average height and its standard deviation can be used to collapse the height probability onto a single curve for any system size. The collapse appeared to be rough, meaning the height does not follow the Central Limit Theorem.

The avalanche-size exponents can be used to perform a data collapse for the avalanche size probability by aligning the characteristic bumps of each system size. This method showed good results, but more analysis is needed for bigger system sizes. The avalanche-size exponents can be measured via two methods: analysing the avalanche-size probability and performing the k'th moment analysis. Both procedures gave consistent results within the error range: $\tau_s \approx 1.54$ and $D \approx 2.15$.

Although the data for the total height and the avalanche sizes can be analysed and collapsed, the theory behind non-equilibrium critical systems remains incomplete.

References

[1] Bak, Per and Tang, Chao and Wiesenfeld, Kurt, *Self-organized criticality: An explanation of the 1/f noise*, 1987. Available from: https://link.aps.org/doi/10.1103/PhysRevLett.59.381 [Accessed: February 2023]

[2] K. Christensen and Nicholas R. Moloney, *Complexity and Criticality*, Imperial College Press, 2005. [Accessed: February 2023]

[3] Schafer R., *What Is a Savitzky-Golay Filter?*, IEEE Signal Processing Magazine, 2011. [Accessed: February 2023]

[4] Trinidad C., *Central Limit Theorem*, Corporate Finance Institute, 2020. Available from: https://corporatefinanceinstitute.com/resources/data-science/central-limit-theorem/ [Accessed: February 2023]

[5] Stephanie Glen, *Kolmogorov-Smirnov Goodness of Fit Test*, StatisticsHowTo, 2022. Available from: https://www.statisticshowto.com/kolmogorov-smirnov-test/ [Accessed: February 2023]